Phase Transitions in the Assembly of Multi-Valent Signaling Proteins

Pilong Li[1,7], **Sudeep Banjade**[1,7], **Hui-Chun Cheng**[1,7], **Soyeon Kim**[1], **Baoyu Chen**[1], **Liang Guo**[2], **Marc Llaguno**[3], **Javoris V. Hollingsworth**[4], **David S. King**[5], **Salman F. Banani**[1], **Paul S. Russo**[4], **Qiu-Xing Jiang**[3], **B. Tracy Nixon**[6], and **Michael K. Rosen**[1]

[1]Department of Biochemistry and Howard Hughes Medical Institute, UT Southwestern Medical Center, Dallas, TX 75390-8812, USA

[2]BioCAT of IIT at the Advanced Photon Source, Argonne National Laboratory, 9700 South Cass Avenue, Argonne, Illinois 60439, USA

[3]Department of Cell Biology, University of Texas Southwestern Medical Center, Dallas, TX 75390-9148, USA

[4]Department of Chemistry and Macromolecular Studies Group, Louisiana State University, Baton Rouge, Louisiana 70803, USA

[5]Howard Hughes Medical Institute Mass Spectrometry Laboratory and Department of Molecular & Cell Biology, University of California, Berkeley, CA 94720, USA

[6]Department of Biochemistry and Molecular Biology, The Pennsylvania State University, University Park, PA 16802, USA

Abstract

Cells are organized on length scales ranging from Angstroms to microns. However, the mechanisms by which Angstrom-scale molecular properties are translated to micron-scale macroscopic properties are not well understood. Here we show that interactions between diverse, synthetic multivalent macromolecules (including multi-domain proteins and RNA) produce sharp, liquid-liquid demixing phase separations, generating micron-sized liquid droplets in aqueous solution. This macroscopic transition corresponds to a molecular transition between small complexes and large, dynamic supramolecular polymers. The concentrations needed for phase transition are directly related to valency of the interacting species. In the case of the actin

Correspondence to Michael K. Rosen: Michael.Rosen@utsouthwestern.edu Telephone: 214-645-6361.
[7]Equal contributions

regulatory protein, neuronal Wiskott-Aldrich Syndrome Protein (N-WASP) interacting with its established biological partners Nck and phosphorylated nephrin[1], the phase transition corresponds to a sharp increase in activity toward the actin nucleation factor, Arp2/3 complex. The transition is governed by the degree of phosphorylation of nephrin, explaining how this property of the system can be controlled to regulatory effect by kinases. The widespread occurrence of multivalent systems suggests that phase transitions are likely used to spatially organize and biochemically regulate information throughout biology.

Covalent and non-covalent interactions between multivalent small molecules are central elements of classical polymer chemistry/physics and supramolecular chemistry[2,3,4]. These fields have produced theories and experimental demonstrations of sharp transitions between small assemblies and macroscopic polymer gels (sol-gel transitions) as the degree of bonding increases. The transition point (critical point) depends on physical properties of the monomeric species such as valency and affinity. The polymer can have a variety of physical forms, ranging from phase-separated liquid to crystalline solid. For non-covalent systems, phase separation can strongly influence the sol-gel transition by altering the degree of bonding[5,6]. In biology, interactions between multivalent entities are found in many processes, ranging from extracellular carbohydrate-lectin binding to intracellular signaling to RNA metabolism to chromatin organization in the nucleus[7,8,9,10]. Biological multivalency has been studied most extensively in the context of extracellular ligands binding to cell surface receptors, where antibody-receptor[11] and carbohydrate-lectin[7] systems can assemble into crosslinked networks. These networks are typically precipitates[11,12], but liquid-like gels have also been described[13]. Multivalency has been less studied in the context of intracellular molecules, which often share characteristics of high valency, modest affinity and long, flexible connections between binding elements[14]. Here we asked whether these systems also undergo sharp transitions to polymer, and if so, what the macroscopic properties of the polymer are, and how such transitions could be regulated and affect function.

Initially we examined interactions between the Src homology 3 (SH3) domain and its proline-rich motif (PRM) ligand, two widely observed modules that often appear in tandem arrays in signaling proteins[8,14]. We generated two classes of engineered proteins, one composed of repeats of a single SH3 domain ($SH3_m$, m=1–5) and a second composed of repeats of a PRM ligand (PRM_n, n=1–5; $K_D = 350$ μM for the $SH3_1$-PRM_1 interaction; Supplementary Fig. 1). Initially we mixed $SH3_4$ with PRM_4. At low concentrations the solutions were clear, while at high concentrations they were opalescent. Examination of such opalescent solutions using light microscopy revealed the presence of numerous spherical droplets, ~1 μm to >50 μm in diameter, that had phase separated from the bulk solution (Fig. 1a, Supplementary Fig. 2). Smaller droplets tended to coalesce into larger droplets over time, consistent with liquid-like properties (Fig. 1b). When the proteins were mixed in 1:1 ratio, both the droplet and bulk phases contained equal amounts of each molecule. But the proteins are concentrated ~100-fold in the droplets relative to the bulk (Fig. 1a, right; 116-fold for $SH3_5$+PRM_5, 82-fold for a $SH3_5$ plus an octameric dendrimer, $PRM(N-WASP)_8$). Analogous droplets were also observed with an unrelated $SH3_5$-$ligand_5$ pair and with the tetravalent RNA binding protein, PTB, interacting with an RNA

oligonucleotide (Supplementary Fig. 3). Thus, liquid-liquid demixing phase transitions may be widely observed in intracellular multivalent systems.

A large body of data indicates that the phase separation observed here is driven by assembly of the multivalent proteins into large species, analogous to behavior observed in many small molecule polymer systems[2,5] and also with covalent protein crosslinking[15]. First, the phase boundary is strongly dependent on valency of the interacting species (Fig. 2a, Supplementary Fig. 4). This observation is consistent with theory and our simulations, which indicate that higher valency enables formation of larger species at lower fractional saturation of binding modules[2,3,5,16] (Supplementary Simulations and Theory, Supplementary Figs. 5–7). Second, the phase transition can be blocked by a high affinity monovalent ligand, $PRM(H)_1$ ($K_D = 10$ μM for $SH3_1$ binding $PRM(H)_1$; Supplementary Fig. 8). Third, we used dynamic light scattering (DLS) and small angle x-ray scattering (SAXS) to characterize the species formed during titrations of PRM proteins into $SH3_5$ (Fig. 2b, Supplementary Figs. 10–12). Below their concentrations needed for droplet formation, both PRM_2 and PRM_4 substantially increased the apparent hydrodynamic radius (R_h, for DLS) and apparent radius of gyration (R_g, for SAXS), suggesting the formation of oligomeric species. For equal total module concentrations, PRM_4 caused larger increases than did PRM_2, consistent with predictions from polymer theory[2,3,5,16]. For higher concentrations, we removed droplets by centrifugation, and found that increasing PRM_2 and PRM_4 caused R_h and R_g to decrease in the bulk phase, suggesting that larger species partitioned selectively into the droplet phase. This behavior resembles that observed in sol-gel transitions of covalent polymers, where above the critical extent of reaction the average size of oligomers in the sol phase decreases, because larger species preferentially join the gel[2]. Titrations with PRM_1 or $PRM(H)_1$, which unlike PRM_2 and PRM_4 cannot generate polymers and did not cause phase separation, produced only small, saturable increases in R_h and R_g. Together these data indicate that phase separation is driven by the unique ability of multivalent $SH3_m$-PRM_n interactions to create large assemblies.

Additional data suggest that the multivalent proteins have formed large polymers within the droplets, such that the phase transition likely coincides with a sol-gel transition. First, at the extremely high concentrations in the droplet phase, the fractional saturation of SH3/PRM binding sites is estimated to be 3–5-fold higher than that needed to induce the sol-gel transition[16] (Supplementary Materials, Cyclization). Second, DLS analyses of droplet phases created by $SH3_m$/PRM_n mixtures showed multi-phasic intensity autocorrelation curves with a complex distribution of relaxation times spanning 0.2–20 ms (Supplementary Fig. 13) or beyond (Fig. 2c). Some of these relaxation times scale non-linearly with the square of scattering angle (q^2, Supplementary Fig. 13). The wide range of timescales, presence of long timescale processes and q^2-independence of some of these processes are typical of polymer solutions in the semi-dilute range, but highly atypical of discrete molecular species[17]. Third, photobleaching studies showed that the diffusion of the droplet constituents is slowed by ~3 orders of magnitude relative to free diffusion in water (not shown). Further, the photobleaching recovery rate correlates inversely with monomer-monomer affinity and valency (Supplementary Fig. 14), suggesting that recovery represents reorganization of a polymer matrix. Small molecule fluorophores and EGFP can enter and move rapidly within the droplets (Supplementary Fig. 15). Finally, electron cryo-

microscopic images of SH3$_5$+PRM$_5$ solutions flash frozen immediately after mixing showed numerous round, electron dense objects with diameters of 50~500 nm (Fig. 2d; Supplementary Fig. 16). These objects were not observed with high concentrations of either SH3$_5$ or PRM$_5$ alone, or with the two components mixed below the droplet concentration. Although the objects were too dense to observe structures within them, their edges were highly irregular on the ~10 nm scale, suggesting they contained large but disordered molecular species, consistent with a crosslinked gel. These characterizations of the droplet phase suggest that it contains large polymeric species and likely has undergone a sol-gel transition.

Together our data suggest a model in which association of multivalent proteins produces macroscopic liquid-liquid phase separation, which is thermodynamically coupled to a molecular sol-gel transition within the droplet phase. The sharp transition between small complex and polymer is consistent with condensation polymerization theory[2,3,6], and our own particle-based simulations (Supplementary Fig. 5). A theoretical analysis of these systems (Supplementary Simulations and Theory) indicates that the polymerization process is driven appreciably by the extremely high configurational entropy of the polymer[6,18].

The behavior we observe for these multivalent systems *in vitro* is mirrored in cells. Co-expression of mCherry-SH3$_5$ and eGFP-PRM$_5$ in HeLa cells results in formation of 0.5~2 μm diameter, cytoplasmic puncta containing both fluorophores (Fig. 3a). Puncta are not observed in cells expressing either protein alone, or in cells co-expressing mCherry-SH3$_5$ + eGFP-PRM$_3$, indicating that their formation is dependent on interaction between the two high-valent molecules. The puncta do not stain with a large range of vesicle markers or a lipid dye, suggesting they are phase-separated bodies rather than vesicular structures (Supplementary Fig. 18). Both mCherry and eGFP fluorescence of the bodies recover in ~10 seconds after photobleaching (Fig. 3b), indicating rapid exchange of both components with the surrounding cytoplasm and suggesting a dynamic, liquid-like nature. Thus, interactions between multi-valent proteins can produce phase separated liquid droplets both *in vitro* and in cells.

The nephrin/Nck/N-WASP system constitutes a natural, three-component interaction to investigate phase transitions resulting from multi-valent interactions, and their functional consequences (Fig. 4a). In kidney podocytes, the transmembrane protein nephrin plays a central role in forming the glomerular filtration barrier, acting partly through assembling cortical actin[1]. The cytoplasmic tail of nephrin contains three tyrosine phosphorylation (pY) sites, which can each bind the SH2 domain of Nck[1,19]. Nck contains three SH3 domains which can bind the ~six PRMs in the proline-rich region of N-WASP[20]. N-WASP, in turn stimulates actin filament nucleation by the Arp2/3 complex. Multivalency in nephrin or Nck is necessary for proper actin assembly[19], and together with multivalency in N-WASP has potential to cause phase transitions.

Addition of Nck to an N-WASP construct (GBD-P-VCA, Supplementary Table 1; called N-WASP hereafter) causes droplet formation as in the model systems above (Fig. 4b). Addition of a di-phosphorylated nephrin tail peptide (2pY) drops the phase boundary for both proteins by 2-fold (Fig. 4c), presumably because the effective valency of Nck

increases when arrayed on nephrin. This effect is even more pronounced when nephrin 3pY peptide is added (to the same total pY concentration) (Fig. 4d). Thus, in cells kinases could regulate phase transitions in this system (and cooperative assembly of all three proteins) by controlling the degree of phosphorylation of nephrin, and consequently shifting the phase boundary from μM (Fig. 4b) to nM (Fig. 4d) regimes. We note that where measured, the cytoplasmic concentrations of WASP and other actin regulatory proteins are typically 1-10 μM, indicating that shifts in this range could be functionally important (Supplementary Fig. 19).

We next asked how droplet formation affects the ability of the nephrin/Nck/N-WASP system to stimulate Arp2/3-mediated actin assembly. We measured the half time to completion ($t_{1/2}$) of pyrene-actin assembly reactions containing fixed concentrations of the Arp2/3 complex, Nck, nephrin 3pY peptide and N-WASP, plus variable amounts of an N-WASP truncation mutant (N-WASP) that contains the full proline-rich region, can assemble into polymers, but cannot bind the Arp2/3 complex. In the absence of N-WASP , the 50 nM N-WASP produces only weak stimulation of the Arp2/3 complex (long $t_{1/2}$) (Fig. 4e). Addition of N-WASP to concentrations between 0–750 nM has no effect on actin assembly. But 1000 nM N-WASP sharply increases activation of the Arp2/3 complex. Activity increases asymptotically as N-WASP is further raised. N- WASP has no effect on an N-WASP protein that lacks the proline-rich region, suggesting that engagement by Nck is needed for the enhancement of activity (Supplementary Fig. 20). These data are consistent with switch-like formation of a higher activity[21,22], likely polymeric, form of nephrin/Nck/N-WASP when the total concentration of wild type (active) plus truncated (inactive) N-WASP surpasses that needed for droplet formation. The sharp transition is followed by slower increases in activity as additional N-WASP draws a greater percentage of the wild type protein into the droplets/polymer. Consistent with these ideas, when reactions containing N-WASP above its phase separation concentration are stained with phalloidin, numerous actin filament bundles are observed within the droplets (Fig. 4f). In cells, nephrin is transmembrane, and the system would produce not a three dimensional polymer phase as observed here, but rather its two dimensional equivalent at the plasma membrane. Such interactions may contribute to formation and/or stability of the micron-scale clusters of nephrin and Nck, with associated actin tails, which are observed in cells upon nephrin crosslinking (and consequent phosphorylation)[1]. Of the 28 known binding partners of the Nck SH2 domain, 14 are predicted or demonstrated to contain three or more pY binding sites[23,24], suggesting that analogous pY/Nck/N-WASP assembly may occur in many systems.

Sharp phase transitions occurring concomitantly with sol-gel transitions may be a general feature of multivalent systems in biology. Many "cellular bodies" — sub-cellular compartments that are compositionally distinct from the surrounding cytoplasm or nucleoplasm, but are not membrane-bound[25,26] – are enriched in multivalent proteins and nucleic acids[9,27]. These include promyelocytic leukemia nuclear bodies, Cajal bodies, P bodies and P granules[27,28,29]. Moreover, P granules in the *C. elegans* embryo were recently shown to have liquid-like properties with many of the features that we have observed here, including switch-like formation and greatly slowed diffusion of constituent molecules[30].

Many multivalent proteins in general can organize into puncta in the cytosol or at membranes (Supplementary Fig. 21). Within these objects the physical properties of a polymer could impart micron-scale structural and dynamic organization, and control chemistry (e.g. catalysis, interactions, structural rearrangements). Our findings provide a mechanism by which multivalent interactions could potentially yield sharp transitions between physically and functionally distinct states, generating non-linearity in signaling pathways, connecting disparate length scales in the cell, and perhaps contributing to the structure and function of cellular bodies and other two- and three-dimensional compartments.

Methods Summary

Material generation

See Supplementary Materials.

In vitro phase separation

Samples were incubated for >12 hours before scoring for droplets using bright-field microscopy; when observed, droplets formed immediately after mixing. For *in vitro* FRAP experiments, a 5 μm diameter spot was bleached in OG-SH3$_4$-containing droplets >20 μm in diameter using a 488 nm laser line. Mean intensity of the bleached spot was fit to a single exponential.

DLS and SAXS

For titrations monitored by DLS (DynaPro, Wyatt) and SAXS (Advanced Photon Source, BioCAT beamline), samples contained 170 μM SH3$_5$ plus PRM proteins at PRM:SH3 module ratios of 0–5. Droplets were removed from all relevant samples by centrifugation (16,000 g, 10 minutes) before analysis. For SH3$_5$+PRM(N-WASP)$_8$ and SH3$_5$+PRM$_5$ droplets, single angle DLS data were collected on a DynaPro instrument (Wyatt), and multi-angle DLS data were collected on a custom build apparatus, respectively.

Electron cryo-microscopy

Samples were blotted and frozen immediately after mixing, and imaged under low-dose cryo conditions in a JEOL 2200FS FEG transmission electron microscope, using a 2Kx2K Tietz slowscan CCD camera.

Cellular assays

HeLa cells were imaged at 32 °C 24 hours after transfection with vectors expressing mCherry-SH3$_5$ and/or eGFP-PRM$_5$ (or eGFP-PRM$_3$). Images were acquired on a Zeiss LSM 510 confocal microscope. For FRAP experiments, individual mCherry-SH3$_5$/eGFP-PRM$_5$ puncta were bleached with a 488 nm laser line.

Actin polymerization

4 μM actin (5% pyrene labeled) was polymerized in the presence of 3 μM nephrin 3pY, 10 μM Nck, 50 nM N-WASP, and 10 nM Arp2/3 complex plus increasing concentrations of N-

WASP in 150KMEI buffer as described[21]. Imaging was performed on a Zeiss LSM 510 confocal microscope after adding rhodamine-actin (10 % labeled, 4 μM), 300 nM Alexa 488 phalloidin and 10 nM Arp2/3 complex to droplets containing 3 μM nephrin 3pY, 10 μM Nck and 2 μM N-WASP.

Supplementary Material

Refer to Web version on PubMed Central for supplementary material.

Acknowledgments

References

1. Jones N, et al. Nck adaptor proteins link nephrin to the actin cytoskeleton of kidney podocytes. Nature. 2006; 440:818–823. [PubMed: 16525419]

2. Flory, PJ. Principles of Polymer Chemistry. Cornell University Press; 1953.

3. Cohen RJ, Benedek GB. Equilibrium and Kinetic Theory of Polymerization and the Sol-Gel Transition. J Phys Chem. 1982; 86:3696–3714.

4. Lehn JM. Supramolecular Polymer Chemistry--Scope and Perspectives. Polym Int. 2002; 51:825–839.

5. Tanaka, F. Polymer Physics: Applications to Molecular Association and Thermoreversible Gelation. Cambridge University Press; 2011.

6. Semenov AN, Rubinstein M. Thermoreversible gelation in solutions of associative polymers. 1 Statics. Macromolecules. 1998; 31:1373–1385.

7. Brewer CF, Miceli MC, Baum LG. Clusters, bundles, arrays and lattices: novel mechanisms for lectin-saccharide-mediated cellular interactions. Curr Opin Struct Biol. 2002; 12:616–623. [PubMed: 12464313]

8. Pawson T, Nash P. Assembly of cell regulatory systems through protein interaction domains. Science. 2003; 300:445–452. [PubMed: 12702867]

9. Lunde BM, Moore C, Varani G. RNA-binding proteins: modular design for efficient function. Nat Rev Mol Cell Biol. 2007; 8:479–490. [PubMed: 17473849]

10. Ruthenburg AJ, Li H, Patel DJ, Allis CD. Multivalent engagement of chromatin modifications by linked binding modules. Nat Rev Mol Cell Biol. 2007; 8:983–994. [PubMed: 18037899]

11. Goldberg R. A theory of antibody-antigen reactions. I Theory for reactions of multivalent antigen with bivalent and univalent antibody. J Am Chem Soc. 1952; 74:5715–5725.

12. Dam TK, et al. Thermodynamic, kinetic, and electron microscopy studies of concanavalin A and Dioclea grandiflora lectin cross-linked with synthetic divalent carbohydrates. J Biol Chem. 2005; 280:8640–8646. [PubMed: 15632152]

13. Sisu C, et al. The influence of ligand valency on aggregation mechanisms for inhibiting bacterial toxins. Chembiochem. 2009; 10:329–337. [PubMed: 19034953]

14. Jin J, et al. Eukaryotic protein domains as functional units of cellular evolution. Sci Signal. 2009; 2:ra76. [PubMed: 19934434]

15. Asherle N, et al. Oligomerization and phase separation in globular protein solutions. Biophys Chem. 1998; 75:213–227. [PubMed: 9894340]

16. Stockmayer WH. Molecular Distribution in Condensation Polymers. J Polymer Sci. 1952; 9:69–71.

17. Li J, Ngai T, Wu C. The Slow Relaxation Mode: From Solutions to Gel Networks. Polym J. 2010; 42:609–625.

18. Semenov A, Charlot A, Auzely-Velty R, Rinaudo M. Rheological properties of binary associating polymers. Rheologica Acta. 2007; 46:541–568.

19. Blasutig IM, et al. Phosphorylated YDXV motifs and Nck SH2/SH3 adaptors act cooperatively to induce actin reorganization. Mol Cell Biol. 2008; 28:2035–2046. [PubMed: 18212058]

20. Rohatgi R, Nollau P, Ho HY, Kirschner MW, Mayer BJ. Nck and phosphatidylinositol 4,5-bisphosphate synergistically activate actin polymerization through the N-WASP-Arp2/3 pathway. J Biol Chem. 2001; 276:26448–26452. [PubMed: 11340081]

21. Padrick SB, et al. Hierarchical regulation of WASP/WAVE proteins. Mol Cell. 2008; 32:426–438. [PubMed: 18995840]

22. Padrick SB, Rosen MK. Physical mechanisms of signal integration by WASP family proteins. Annu Rev Biochem. 2010; 79:707–735. [PubMed: 20533885]

23. Lettau M, Pieper J, Janssen O. Nck adaptor proteins: functional versatility in T cells. Cell Communication and Signaling. 2009; 7:1. [PubMed: 19187548]

24. Obenauer JC, Cantley LC, Yaffe MB. Scansite 2.0: Proteome-wide prediction of cell signaling interactions using short sequence motifs. Nucleic Acids Res. 2003; 31:3635–3641. [PubMed: 12824383]

25. Matera AG, Izaguire-Sierra M, Praveen K, Rajendra TK. Nuclear bodies: random aggregates of sticky proteins or crucibles of macromolecular assembly? Dev Cell. 2009; 17:639–647. [PubMed: 19922869]

26. Buchan JR, Parker R. Eukaryotic stress granules: the ins and outs of translation. Mol Cell. 2009; 36:932–941. [PubMed: 20064460]

27. Parker R, Sheth U. P bodies and the control of mRNA translation and degradation. Mol Cell. 2007; 25:635–646. [PubMed: 17349952]

28. Matera AG, Shpargel KB. Pumping RNA: nuclear bodybuilding along the RNP pipeline. Curr Opin Cell Biol. 2006; 18:317–324. [PubMed: 16632338]

29. Bernardi R, Pandolfi PP. Structure, dynamics and functions of promyelocytic leukaemia nuclear bodies. Nat Rev Mol Cell Biol. 2007; 8:1006–1016. [PubMed: 17928811]

30. Brangwynne CP, et al. Germline P granules are liquid droplets that localize by controlled dissolution/condensation. Science. 2009; 324:1729–1732. [PubMed: 19460965]
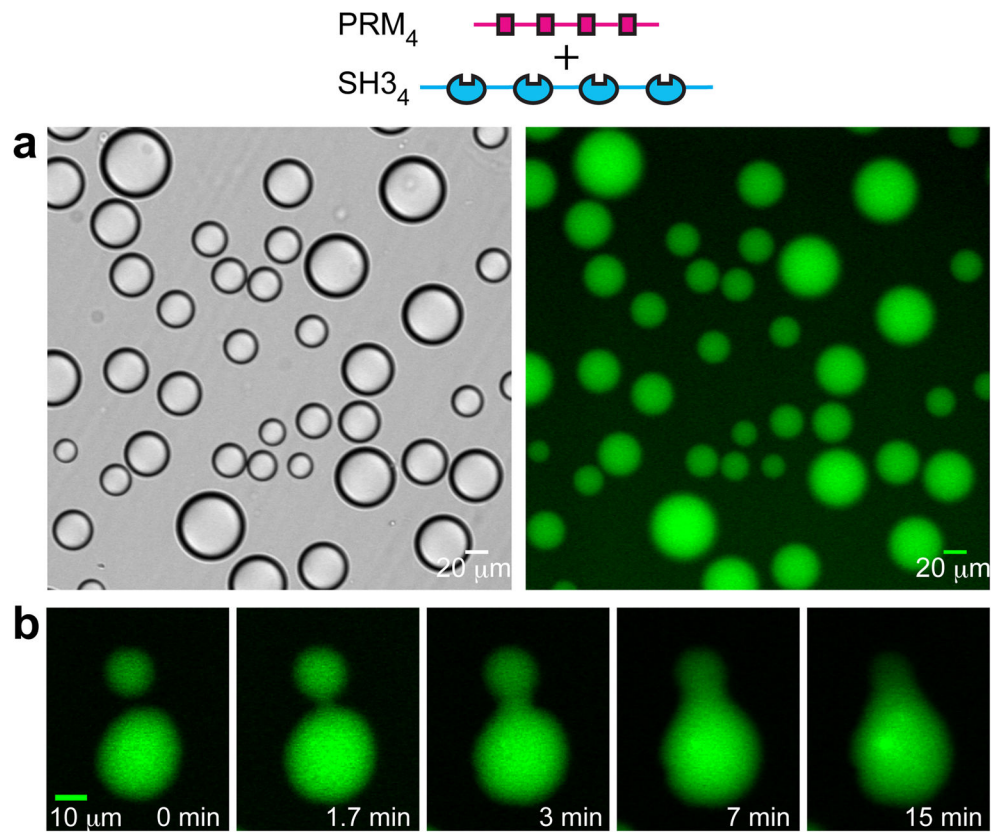
Figure 1. Macroscopic and microscopic phase transitions in multivalent SH3+PRM systems
a, Liquid droplets observed by differential interference contrast microscopy (left) and widefield fluorescence microscopy (right) when 300 μM SH3$_4$, 300 μM PRM$_4$ (module concentrations; molecule concentrations are 75 μM) and 0.5 μM OG-SH3$_4$ are mixed. **b,** Time-lapse imaging of merging droplets formed as in **a**.
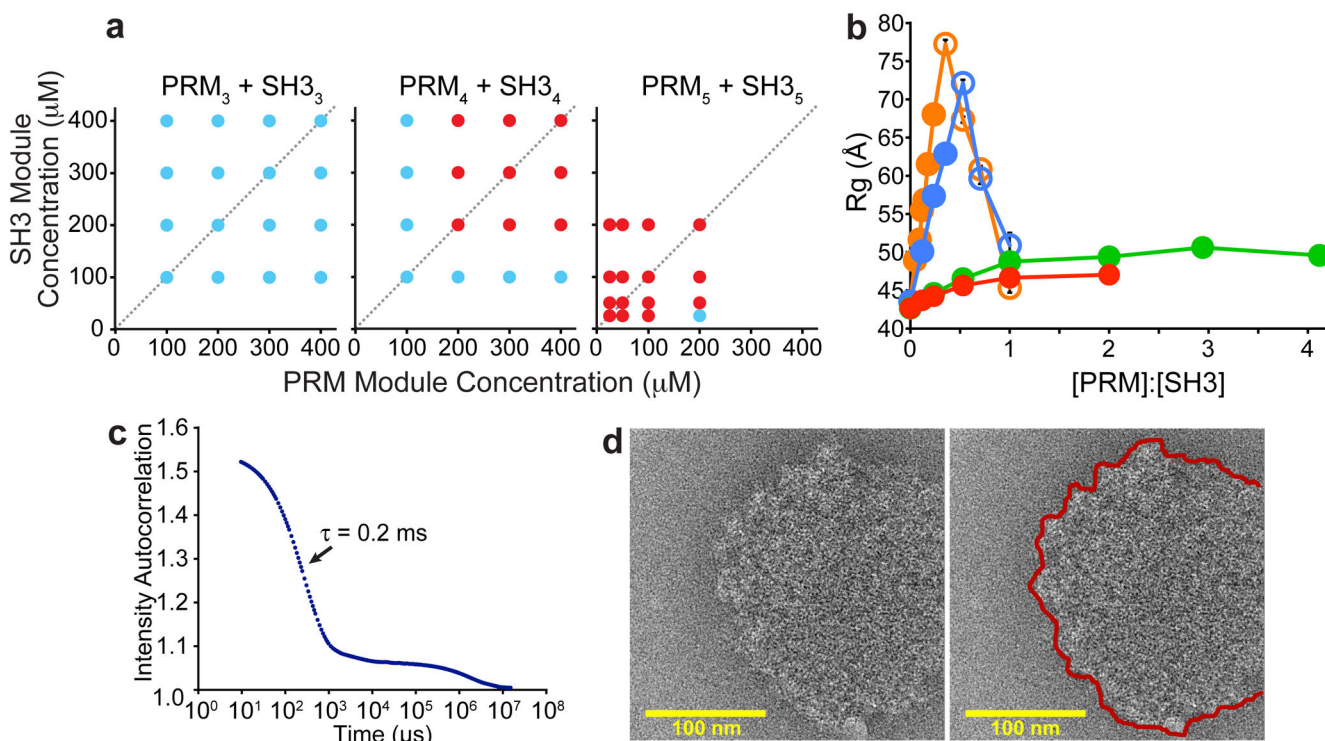
Figure 2. Multivalency drives phase separation and likely a sol-gel transition in the droplet phase
a, Phase diagrams of multivalent SH3 and PRM proteins. Concentrations are in terms of modules. Red and blue circles indicate phase separation and no phase separation, respectively. **b.** R_g values determined from SAXS data collected during titrations of PRM proteins into $SH3_5$. Closed circles indicate the absence of phase separation; open circles indicate data collected on supernatant phase, separated from droplets by centrifugation. Titrations used PRM_4 (orange), PRM_2 (blue), PRM_1 (green), $PRM(H)_1$ (red). Error bars represent standard deviation calculated from 5- 10 independent measurements of I versus Q. **c.** Intensity autocorrelation curve of light scattered at 90 ° from the pooled droplet phase of $SH3_5 + PRM(N-WASP)_8$. **d.** Electron cryo-microscopic image of a droplet formed by $SH3_5 + PRM_5$. Right panel shows edge of the structure with a red line.
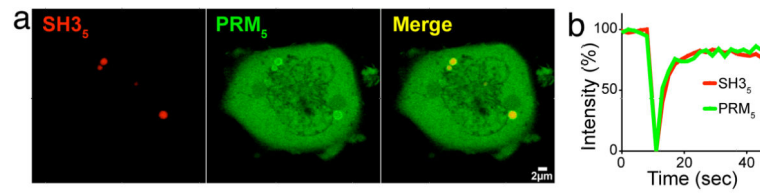
Figure 3. Co-expression of SH3$_5$ and PRM$_5$ in cells produces dynamic puncta
a, From left to right, panels show mCherry-SH3$_5$, eGFP-PRM$_5$ and overlay in a cell expressing both proteins. Note that non-uniform eGFP fluorescence in the puncta is due to mCherry-eGFP FRET rather than differential localization of the proteins (Supplementary Fig. 17). **b,** Both mCherry and eGFP fluorescence recover rapidly after photobleaching.
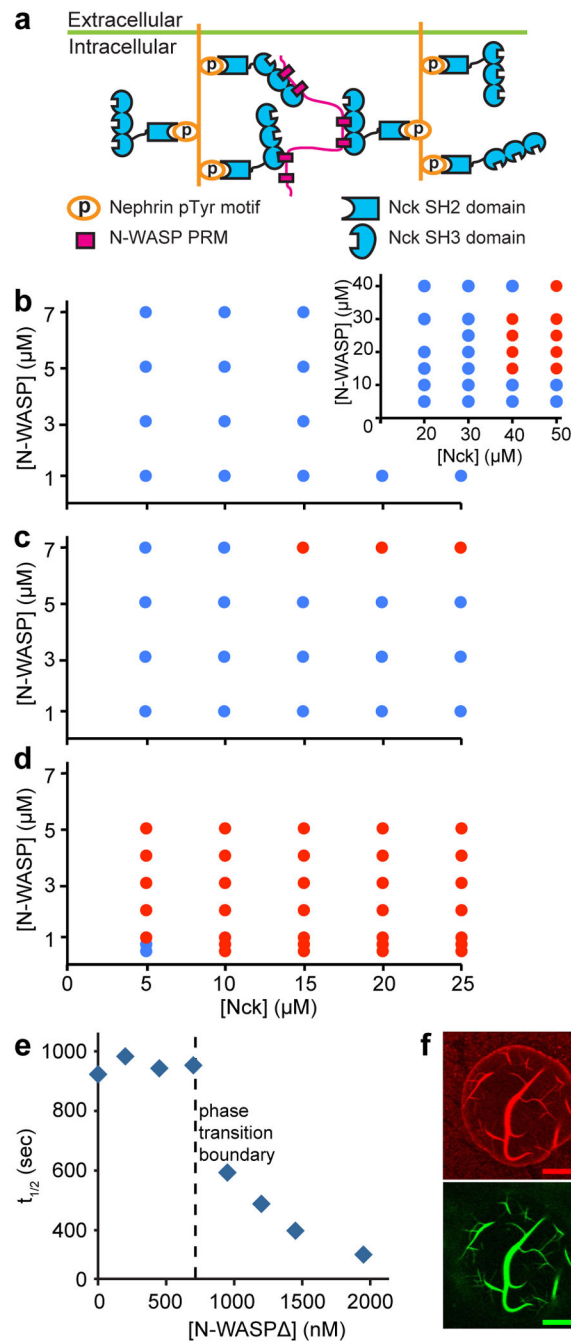
Figure 4. Phase transition correlates to biochemical activity transition in the nephrin/Nck/N-WASP system

a, Interactions of nephrin, Nck and N-WASP. **b-d**, Phase diagrams of N-WASP and Nck alone (**b**) or in the presence of 4.5 μm doubly- (**c**) or 3 μm triply-phosphorylated (**d**) nephrin tail peptides. Red and blue circles same as in Figure 2a. **e**, Half-time ($t_{1/2}$) of N-WASP-stimulated actin assembly by the Arp2/3 complex as a function of N-WASP concentration. Vertical dashed line indicates the phase separation boundary determined in separate assays without actin and Arp2/3 complex. **f**, Rhodamine-actin (10 % labeled, 4 μM), 300 nM Alexa

488–phalloidin and 10 nM Arp2/3 complex were added to droplets containing triply-phosphorylated nephrin, Nck and N-WASP and imaged by confocal microscopy. Top panel = rhodamine; bottom panel = Alexa 488. Scale bar = 10 μm.